Valence-State Atoms in Molecules. 7. Influence of Polarization and Bond-Charge on Spectroscopic Constants of Diatomic Molecules

ARTICLE *in* THE JOURNAL OF PHYSICAL CHEMISTRY A · DECEMBER 2003

Impact Factor: 2.69 · DOI: 10.1021/jp035902b

3 AUTHORS, INCLUDING:

Willem Mulder
The University of the West Indies at Mona
49 PUBLICATIONS **601** CITATIONS
SEE PROFILE

Laszlo von szentpaly
Universität Stuttgart
66 PUBLICATIONS **3,221** CITATIONS
SEE PROFILE

Valence-State Atoms in Molecules. 7. Influence of Polarization and Bond-Charge on Spectroscopic Constants of Diatomic Molecules

Kelling J. Donald,[†] Willem H. Mulder,[†] and László von Szentpály*,[‡]

Department of Chemistry, University of the West Indies, Kingston 7, Jamaica, and Institut für Theoretische Chemie der Universität Stuttgart, Pfaffenwaldring 55, D-70569 Stuttgart, Germany

Received: July 2, 2003; In Final Form: November 13, 2003

The polarizable valence-state-atoms-in-molecules (pVSAM) model describes the electron-pair bond in A−B molecules by superposing core-polarized A^+B^-, A^-B^+, and A:B structures, whose weights are determined by electronegativity equalization. The polarizable valence state potential energy curve (pVS-PEC) is derived through the systematic improvement of the valence state potential energy curve (VS-PEC) [Gardner, D. O. N.; von Szentpály, L. *J. Phys. Chem. A* **1999**, *103*, 9313] and is given as $U(R) = -[(K_1/R) + (K_2/R^4) + (K_3/R^7)] + (T/R)\exp(-\lambda R)$. The first bracketed term contains the Coulomb, charge-induced dipole, and induced dipole−induced dipole terms, derived from weighted ionic and covalent bond-charge contributions. The potential is tested on a broad variety of homonuclear diatoms and heteronuclear halides and hydrides (a total of 52 molecules). The accuracies of the dimensionless vibration−rotation coupling constant (F) and the anharmonicity constant (G) for the halides of the alkali and coinage metals are significantly better than those of the Morse, Rydberg, simple bond-charge, and Rittner potentials. Adding core polarization to the VS-PEC reduces the average unsigned errors in the spectroscopic constants of 47 diatomic molecules from 17.1% to 7.5% in F and 18.9% to 7.8% in G, whereas those of the Morse potential amount to 32.6% and 31.4%, respectively.

1. Introduction

Parametrized potential energy curves (PECs) normally reveal serious limits, if tested for their universal applicability and accuracy. The best-known three-parameter empirical curves (e.g., the Morse and Rydberg functions) are universally applicable; however, their average overall accuracy is rather poor, even for the ground state of covalent molecules,[1,2] and they fail badly for very polar systems, such as the alkali-metal halides.[3−5] The seven-parameter Zavitsas function[6] cannot be called universal, because it completely breaks down for very polar molecules.[5,6] The average unsigned error of the Extended Rydberg PEC[7] is ∼10 times larger for the alkali-metal halides than that for covalent molecules.[5] On the other hand, the Rittner PEC, or polarized-ion model,[8] is successful in calculating the spectroscopic data and dipole moments of the alkali-metal halides. We have most recently extended the polarized-ion model to include quadrupole effects in the calculation of alkaline-earth and group 12 dihalides (AB_2).[8b] However, the Rittner model, and its extensions, exclude charge equilibration and bond formation by shared electron pairs; the model is strictly limited to the extreme ionic case A^+B^- and additionally requires that both the cationic and anionic polarizability volumes ($\alpha' = \alpha/(4\pi\epsilon_o)$) are less than $(4\pi/3)R_e^3$, where α is the static dipole polarizability and R_e is the equilibrium bond distance. This requirement is rarely fulfilled; starting from the alkali-metal hydrides and alkaline-earth monohalides, there are many classes of molecules for which the Rittner model cannot be applied. Bridging the gap by a model that combines the advantages of both the extreme ionic and covalent standpoints would be very gratifying.

One of us and colleagues[3−5,9−12] developed the valence-state-atoms-in-molecules (VSAM) model of bonding as a step toward a universal PEC. The basic idea is to model the structural components in the molecule as a mixture of hybridized atoms and ions, and to determine the asymptotic reference energy, by keeping the ratio of covalent and ionic structures frozen during a constrained dissociation process. Thus, the $1/R$ attraction prevails at long distances and defines the energy of the separated valence-state atoms (VSAs) as promoted above that of ground-state atoms. The $1/R$ asymptote and a sharing−penetration-type valence-state promotion energy form integral parts of the restricted Hartree−Fock model and are discussed in the larger context of Ruedenberg's analysis of chemical bonds.[13] With explicit reference to the simple bond-charge (SBC) model,[14] and Sanderson's overlap argument,[15] the asymptotic $1/R$ dependence was generalized for all distances, and a three-parameter valence-state potential energy curve (VS-PEC) was defined:[3,4,11]

$$U(R) = -\frac{C}{R} + \frac{T}{R}\exp(-\lambda R) \tag{1}$$

The parameters are fitted to R_e, the harmonic force constant (k_e), and the valence-state dissociation energy (D_{VS}), which is defined in Section 2 and is discussed together with the solutions for the parameters C, T, and λ (cf. eq 5 later in this work). The VS-PEC successfully reproduces a representative variety of covalent and ionic reference PECs from $R = 0$ up to the Coulson−Fischer transition,[16] i.e., $R \approx 1.6R_e$. The universal scaling property of this three-parameter VS-PEC has been demonstrated,[4] and the transferability of its parameter λ has been shown.[11] A general extension of the validity range to $R \rightarrow \infty$ has been achieved recently by modeling a soft Coulson−Fischer transition.[5] The relative increase of VS-PEC errors for systems with highly polarizable ion cores, notably the heavy alkali-metal

* Author to whom correspondence should be addressed. E-mail: laszlo@theochem.uni-stuttgart.de.
[†] University of the West Indies.
[‡] Institut für Theoretische Chemie der Universität Stuttgart.

10.1021/jp035902b CCC: $27.50
Published on Web 12/31/2003

hydrides, has been tentatively rationalized[4,5] by the increasing importance of core-polarization and core−valence intershell correlation, both of which may be accounted for by a core-polarization potential (CPP).[17,18]

To prove the point, we extend the VS-PEC into a form that takes core polarization into consideration. The polarizable valence-state-atoms-in-molecules (pVSAM) model links the ionic and covalent descriptions of the bond, using the concept of configuration mixing among contributing ionic and covalent (bond-charge) structures within the framework of the valence-state-atoms-in-molecules (VSAM) model. By incorporating polarization terms, a greater degree of accuracy is expected, and the advantage of physical interpretation is maintained, illustrated, and exploited.

2. Methods

2.1. The VS-PEC. The outer branch ($R > R_e$) of the VS-PEC describes a hypothetical dissociation under constraints. Ruedenberg defined the "atoms in the valence state corresponding to a given molecule" as those resulting from a dissociation process, during which the interference-free portions of the electron populations and electron-pair populations are maintained at their molecular levels.[13] As a prerequisite before any application, Ruedenberg's definition requests some high-level calculations of the interference-free one-electron and two-electron densities, and their integrated populations. We bypass the calculation of densities and obtain the orbital populations (n_i) from the principle of valence-state electronegativity (VSEN) equalization, and the observation of zero spin density in closed-shell molecules, which leads to $n_i\uparrow = n_i\downarrow = {}^1/_2 n_i$.[9,12b] We freeze the intra-atomic electron-pair repulsion energy of the molecule by keeping the local spin population at a value of zero and the VSEN constant at its equalized molecular value during the entire dissociation process.[3−5,9−12] The VSEN is dependent on the Mulliken's orbital electronegativity ($\chi_i^o = {}^1/_2(I_v + A_v)$), the one-center electron-pair repulsion energy ($J_i = I_v - A_v$, where $J_i/2 = \eta_i$, which is the valence-state hardness of the active orbital), and the partial charge ($\delta_i = 1 - n_i$); the VSEN is defined as[9]

$$\chi_{VS,i}(\delta_i) = \chi_i^o + \frac{1}{2} J_i \delta_i \tag{2}$$

I_v, which is the valence ionization potential, and A_v, which is the valence electron affinity, are obtained from the relations $I_v = I + p^+ - p^o$ and $A_v = A + p^o - p^-$, where I and A denote the same properties of the ground-state atoms. The terms p^o, p^+, and p^- are the hybridization/promotion energies of the atom, positive ion, and negative ion, respectively, calculated by the method of Pritchard and Skinner.[19] The VSEN equalization principle states that charge is transferred when the bond is formed, until the orbital electronegativities become equalized.

The partial charge (δ_{Ai}) is thus determined as[3,9,12b]

$$\delta_{Ai} = \frac{2(\chi_{Bj}^o - \chi_{Ai}^o)}{J_{Ai} + J_{Bj}} = \frac{\chi_{Bj}^o - \chi_{Ai}^o}{\eta_{Ai} + \eta_{Bj}} \tag{3}$$

where i and j denote the active valence orbitals on atoms A and B, respectively.

The VS dissociation energy, $D_{VS} = U_{VS}(\infty) - U_{VS}(R_e)$, of a single-bonded molecule AB refers to the dissociation into VSAs and is determined using the relation[3]

$$D_{VS} = D_e + \sum\left(E_{hy} + \frac{J}{4}\right) - \frac{(\Delta\chi^o)^2}{J_A + J_B} \tag{4}$$

where D_e is the spectroscopic dissociation energy, and the second term is a sum over the atoms of the single-bonded molecule AB of hybridization energy E_{hy} (including the promotion to the barycenter of spin−orbit split states) and $J/4$. The final term, which is the electronegativity energy ($E_\chi = -(\Delta\chi_o)^2/(J_A + J_B)$), accounts for energy reduction due to charge transfer by VSEN equalization. The VS-PEC parameters C, T, and λ are determined by R_e, k_e, and D_{VS}:

$$\lambda R_e = \frac{k_e R_e^2}{D_{VS}} = z \tag{5a}$$

$$C = D_{VS} R_e (1 + z^{-1}) \tag{5b}$$

$$T = D_{VS} R_e z^{-1} \exp(z) \tag{5c}$$

2.2. Bond-Charge in the VSAM Model. In the articles published so far,[3−5,11] it has not been necessary to partition C into ionic and covalent contributions; for the latter, it was sufficient to refer to bond-charge models in general. To include core polarization, C must account for the ionic and covalent characteristics of the bond separately. The bond energy of the molecule AB is represented as the sum of the contributions due to ionic and covalent structures. For a single-bonded diatomic molecule, the attractive energy of eq 1 ($-C/R$) is approximated by summing normalized contributions of the ionic structures, A^+B^- and A^-B^+, and a covalent A:B structure:

$$C = c_1^2 C_{A^+B^-} + c_2^2 C_{A^-B^+} + c_3^2 C_{A:B} \tag{6}$$

The covalent structure A:B does not contribute to the bond polarity (δ) or the primary dipole moment. We postulate that the ratio c_1/c_2 is determined by δ, which, in turn, is calculated by VS electronegativity equalization, as indicated in eq 3. If $\delta = 0$, the ionic contributions must carry equal weight, which, according to the restricted Hartree−Fock approximation, and our VSAM model, amounts to $c_1^2 = c_2^2 = {}^1/_4$. If atom B becomes more electronegative, the contribution of the A^+B^- configuration increases, at the expense of the A^-B^+ configuration. In the VSAM model, the coefficients are

$$c_1 = \frac{1 + \delta}{2} \tag{7a}$$

$$c_2 = \frac{1 - \delta}{2} \tag{7b}$$

from which it follows that $c_{ion}^2 = c_1^2 + c_2^2 = (1 + \delta^2)/2$, and $c_{cov}^2 = c_3^2 = (1 - \delta^2)/2$ by normalization. Thus, the resulting PEC may be given in the form

$$U = U_{att} + U_{rep} = c_{ion}^2 W_{ion} + c_{cov}^2 W_{cov} + \frac{T}{R}\exp(-\lambda R) \tag{8}$$

where the coefficients c_{ion} and c_{cov} are functions of δ. The repulsive energy (U_{rep}) could be partitioned into ionic and covalent components ($U_{rep,1} + U_{rep,2} + U_{rep,3}$), using different exponential parameters λ_1−λ_3 and pre-exponential factors T_1−T_3 for the different types of ionic and covalent bonding. However, the universal scaling property[4] in the inner branch of the VS-PEC, and the transferability of λ from homonuclear to

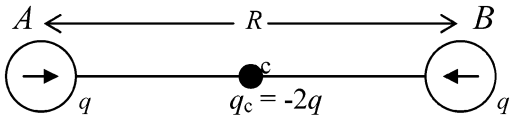

Figure 1. Representation of the covalent configuration in the polarizable valence-state-atoms-in-molecules (pVSAM) model; q_c represents the bond-charge at the bond center, and polarizable cores are located on atoms A and B.

highly ionic diatomic molecules[11] provide more-than-adequate justifications for maintaining the simple two-parameter repulsion "ansatz" with the same λ and T values for all three configurations in eq 6. The screened Coulomb repulsion successfully unifies several types of interactions: (i) the short-range exchange repulsion between closed-shell atomic cores and/or ions, (ii) the distance dependence of the sum of interatomic and on-site electron repulsion energies,[13] and (iii) the increase in electronic kinetic energy of the molecule over that of the separated atoms.[14]

To generate a universal VS-PEC, both W_{ion} and W_{cov} are expressed as summations of terms in $1/R^n$. As a first approximation, W_{ion}, which includes the contributions due to the A^+B^- and A^-B^+ configurations, has been given by the following simple Coulomb expression:

$$W_{ion} = -\frac{e^2}{4\pi\epsilon_o R} \tag{9}$$

for the interaction between two oppositely charged ions at a distance R.

For W_{cov}, we distribute the bonding electron pair between the nuclear positions and the bond center and generate an expression that involves the bond-charge (Figure 1).

The bond-charge is assumed to be due to interference accumulation of electron density. Its distance dependence should be modeled as proportional to the overlap integral; as a first approximation, however, the bond-charge has been assumed to be constant,[14b,c] and we adhere to this simple picture in the vicinity of the equilibrium bond length. The introduction of bond-charges in advancing beyond atom-centered models is also necessary to reproduce the electrostatic potential (ESP) in molecular mechanics.[20] The covalent structure does not contribute to the primary dipole moment; therefore, the A:B bond-charge is generally located at the bond center and contains equal amounts of charge q from both atoms. Thus, we have $-q_c/2 \equiv q$ (cf. Figure 1).

The total energy associated with the system depicted in Figure 1 is approximated as the sum of interactions between the polarized charges at the nuclei and interactions between them and a point charge at the bond center: the derivation is presented in the Appendix. To avoid self-interaction, we allow each atomic center to interact only with the other half of the bond-charge, i.e., the bond-charge fragment $-q$, which is due to the other atomic center. If the Coulomb term included interactions of the atomic centers with the full bond-charge, as done in the SBC model,[14b,c] modeling of the energy that is needed to move the bond-charge from the atomic centers to the bond center would be necessary.

The relevant electrostatic contributions to the binding energy, complete to dipole−dipole interactions, are outlined in the Appendix. Taking only the Coulomb interactions into consideration,

$$W_{cov} = -\frac{3q^2}{4\pi\epsilon_o R} \tag{10}$$

such that (with eqs 7−9)

$$U_{att} = -\left(\frac{1+\delta^2}{2}\right)\frac{e^2}{4\pi\epsilon_o R} - \left(\frac{1-\delta^2}{2}\right)\frac{3q^2}{4\pi\epsilon_o R} \tag{11}$$

The same R dependence in both terms is essential for condensation into a universal three-parameter PEC. However, one must remember that the description of covalent binding by a bond-charge model is a crude approximation,[14b,c] and the "ansatz" $U_{att} = -C/R = -D_{VS}R_e(1 + z^{-1})/R$ is a valid approximation for the attractive portion of a universal PEC in the Coulson−Fischer domain only.[4] The general modeling of a soft Coulson−Fischer transition is described in ref 5. As we focus on the shape of a universal PEC around its minimum, eq 5 is reformulated:

$$C = D_{VS}R_e(1 + z^{-1}) = \left(\frac{1+\delta^2}{2}\right)\frac{e^2}{4\pi\epsilon_o} + \left(\frac{1-\delta^2}{2}\right)\frac{3q^2}{4\pi\epsilon_o} \tag{12}$$

The relationship is consistent with the molecular orbital (MO)−theoretical valence-state formulation, i.e., there are 50% ionic and 50% covalent contributions to the overall potential in the case of homonuclear diatoms.[13] The ionic contributions increase in a conceptually meaningful fashion as δ increases. The bond-charge is evaluated by solving eq 12 for q:

$$q = \left[\frac{8\pi\epsilon_o D_{VS}R_e(1 + z^{-1}) - e^2(1+\delta^2)}{3(1-\delta^2)}\right]^{1/2} \tag{13}$$

An effective bond-charge $q_{c,eff}$ is defined as the product of q_c and the coefficient of the covalent contribution:

$$q_{c,eff} = -2\left(\frac{1-\delta^2}{2}\right)^{1/2} q \tag{14}$$

This polarity-dependent effective bond-charge, $q_{c,eff}$ (with balancing charges $|q_{c,eff}|/2$ at the atomic centers), may be viewed as the charge involved in the interactions that define the covalent contributions to the bonding. In the extreme case where the molecule is completely ionic, the factor $[(1 - \delta^2)/2]^{1/2}$ is reduced to zero and the effective bond-charge disappears.

This prescription will be used to calculate bond-charges for several diatomic molecules, including the alkali and coinage-metal diatoms and the halides and hydrides of group 1 and group 11. Before presenting the results, we introduce an augmented form of the VS-PEC in which the core-polarization contributions are taken into consideration.

2.3. The Polarizable Valence-State-Atoms-in-Molecules (pVSAM) Function. The ionic and covalent components of the energy function in eq 11 may be extended to include polarization terms. For the ionic structures, the interactions may be written in the following familiar form:

$$W_{ion} = -\frac{e^2}{4\pi\epsilon_o}\left(\frac{1}{R} + \frac{\alpha'_A + \alpha'_B}{2R^4} + \frac{2\alpha'_A\alpha'_B}{R^7}\right) \tag{15}$$

In eq 15, the first, second, and third terms result from the Coulomb, charge-induced dipole, and induced dipole−induced dipole interactions, respectively. However, a principal difference from the Rittner model must be considered in eq 15. Rittner's model is limited to the single structure A^+B^-; therefore, an electron pair is strictly localized on B^-, and the relevant polarizability is that of B^-. We assume that the bond is formed by an unequally shared electron pair, whose distribution is sufficiently determined by VSEN equalization; consequently, this pair, or the bond orbital, is not to be further back-polarized

by its own polar distribution, and only the charges that do not contribute to the bond orbital have to be polarized by the latter. Thus, our relevant polarizabilities for A^+B^- *and* A^-B^+ are those of A^+ and B^+. Therefore, in eq 15, α'_B denotes the B^+ cation polarizability volume, to be distinguished from the larger B^- anion polarizability volume, which will be denoted as $\alpha'_{B(-)}$.

Similarly, for the covalent bond-charge term, a system of two polarizable cations at an equal distance from a bond-charge is assumed. Each cation is polarized only by the charge distribution of the other atom: $+q$ at the other nucleus and $-q$ at the bond center.

The energy expression is (see Appendix)

$$W_{cov} = -\frac{3q^2}{4\pi\epsilon_o}\left(\frac{1}{R} + \frac{3(\alpha'_A + \alpha'_B)}{2R^4} - \frac{6\alpha'_A\alpha'_B}{R^7}\right) \quad (16)$$

The three terms on the right-hand side result from the Coulomb, charge-induced dipole (and induced dipole formation), and induced dipole−induced dipole interactions, respectively.

Thus, in accordance with the concept of configuration mixing as modeled in eq 6, and by eqs 15 and 16, the polarizable valence state potential energy curve (pVS-PEC) is defined by the following function:

$$\begin{aligned} U(R) = &-\frac{e^2(1+\delta^2)}{8\pi\epsilon_o}\left(\frac{1}{R} + \frac{(\alpha'_A + \alpha'_B)}{2R^4} + \frac{2\alpha'_A\alpha'_B}{R^7}\right) - \\ &\frac{3q^2(1-\delta^2)}{8\pi\epsilon_o}\left(\frac{1}{R} + \frac{3(\alpha'_A + \alpha'_B)}{2R^4} - \frac{6\alpha'_A\alpha'_B}{R^7}\right) + \frac{T}{R}\exp(-\lambda R) \\ &= U_{ion}(R) + U_{cov}(R) + U_{rep}(R) \\ &= U_{ion}(R) + q^2\Omega_{cov}(R) + \frac{T}{R}\exp(-\lambda R) \end{aligned} \quad (17)$$

where $\Omega_{cov}(R) = U_{cov}(R)q^{-2}$ and the previous attractive term ($-C/R$) is replaced by a function with a more-complex R dependence. Therefore, the number of molecular parameters remains at three, and two polarizabilities are added as fixed atomic parameters. The molecular parameters are determined as usual by R_e, k_e, and $U(\infty) - U(R_e) = D_{VS}$, such that

$$-D_{VS} = U_{ion}(R_e) + q^2\Omega_{cov}(R_e) + \frac{T}{R_e}\exp(-\lambda R_e) \quad (18)$$

At equilibrium, the first and second derivatives of U, with respect to bond length R_e, are

$$\begin{aligned} U'(R_e) &= 0 \\ &= U'_{ion}(R_e) + q^2\Omega'_{cov}(R_e) - \frac{T}{R_e}\exp(-\lambda R_e)\left(\lambda + \frac{1}{R_e}\right) \end{aligned} \quad (19)$$

and

$$\begin{aligned} U''(R_e) &= k_e \\ &= U''_{ion}(R_e) + q^2\Omega''_{cov}(R_e) + \\ &\qquad \frac{T}{R_e}\exp(-\lambda R_e)\left(\lambda^2 + \frac{2\lambda}{R_e} + \frac{2}{R_e^2}\right) \end{aligned} \quad (20)$$

From eq 18, we find

$$T = -(D_{VS} + U_{ion}(R_e) + q^2\Omega_{cov}(R_e))R_e\exp(\lambda R_e) \quad (21)$$

which, according to eq 19, gives

$$q = \left[\frac{-(D_{VS} + U_{ion}(R_e))(\lambda + R_e^{-1}) - U'_{ion}(R_e)}{\Omega'_{cov}(R_e) + \Omega_{cov}(R_e)(\lambda + R_e^{-1})}\right]^{1/2} \quad (22)$$

By substituting for T and q in eq 20, a solution for λ is found, which has the following form:

$$\lambda = \frac{-t + \sqrt{t^2 - 4su}}{2s} \quad (23)$$

where, for $R = R_e$,

$$s = U'_{ion}\Omega_{cov} - (D_{VS} + U_{ion})\Omega'_{cov} \quad (24)$$

$$t = \frac{2s}{R_e} - (D_{VS} + U_{ion})\Omega''_{cov} + (U''_{ion} - k_e)\Omega_{cov} \quad (25)$$

$$u = \frac{t}{R_e} - U'_{ion}\Omega''_{cov} + (U''_{ion} - k_e)\Omega'_{cov} \quad (26)$$

It is now possible to calculate λ and, by substitution into eqs 22 and 21, determine q and T, respectively. If the polarization terms in U_{att} are set to zero, eq 22 simplifies to eq 13. Thus, by eqs 18−26, we can determine all three parameters for the cases with and without polarization contributions.

2.4. Higher Spectroscopic Constants. Having fitted the parameters of the model to D_{VS}, R_e, and k_e, we can calculate values for the rotation−vibration coupling (α_e) and the anharmonicity constant ($\tilde{\nu}_e x_e$). The merits of the pVS-PEC are tested by comparison with the VS-PEC, Morse,[21] Rydberg,[22] and Rittner[8] functions and the experiment.[23,24] It is advantageous to use the dimensionless, isotope-independent expression of these spectroscopic constants, as given in refs 1 and 2:

$$F = -\left(\frac{XR_e}{3} + 1\right) = \frac{\alpha_e\tilde{\nu}_e}{6B_e^2} \quad (27)$$

$$G = R_e^2\left(\frac{5X^2}{3} - Y\right) = \frac{8\tilde{\nu}_e x_e}{B_e} \quad (28)$$

where $X = U'''(R_e)/U''(R_e)$ and $Y = U''''(R_e)/U''(R_e)$. B_e is the equilibrium rotational constant, $\tilde{\nu}_e$ is the harmonic vibrational wavenumber, and F and G are the dimensionless forms of the rotation−vibration coupling α_e and the anharmonicity constant $\tilde{\nu}_e x_e$, respectively. For the VS-PEC, it has been shown that $F = z/3$ and $G = 2z^2/3 + 6z + 3$.[3]

The F and G values can be similarly determined for the pVS-PEC, where

$$U'''(R_e) = U'''_{att}(R_e) - \frac{T}{R_e}\exp(-\lambda R_e)\left(\lambda^3 + \frac{3\lambda^2}{R_e} + \frac{6\lambda}{R_e^2} + \frac{6}{R_e^3}\right) \quad (29)$$

$$\begin{aligned} U''''(R_e) = &U''''_{att}(R_e) + \\ &\frac{T}{R_e}\exp(-\lambda R_e)\left(\lambda^4 + \frac{4\lambda^3}{R_e} + \frac{12\lambda^2}{R_e^2} + \frac{24\lambda}{R_e^3} + \frac{24}{R_e^4}\right) \end{aligned} \quad (30)$$

As already shown (see eq 17), U_{att} has the form

$$U_{att} = -\left(\frac{K_1}{R} + \frac{K_2}{R^4} + \frac{K_3}{R^7}\right) \quad (31)$$

for which the first four derivatives, at $R = R_e$, can be readily evaluated.

Using eqs 20 and 27−30, and the definition $z = \lambda R_e$, it can be shown that

$$F = -\frac{(R_e/3)U'''_{att}(R_e) + U''_{att}(R_e) - [z^3 U_{rep}(R_e)/(3R_e^2)]}{U''_{att}(R_e) + (U_{rep}(R_e)/R_e^2)(z^2 + 2z + 2)} \quad (32)$$

and

$$G = \frac{5R_e^2}{3}\left(\frac{U'''_{att}(R_e) - (U_{rep}(R_e)/R_e^3)(z^3 + 3z^2 + 6z + 6)}{U''_{att}(R_e) + (U_{rep}(R_e)/R_e^2)(z^2 + 2z + 2)}\right)^2 - \frac{R_e^2 U''''_{att}(R_e) + (U_{rep}(R_e)/R_e^2)(z^4 + 4z^3 + 12z^2 + 24z + 24)}{U''_{att}(R_e) + (U_{rep}(R_e)/R_e^2)(z^2 + 2z + 2)} \quad (33)$$

A summary of the solutions for F and G for the Morse and Rydberg functions are provided in refs 1 and 2, and a summary of the solutions for the Rittner function is given in ref 25.

The Rittner function is used in the form

$$U(R) = A\exp\left(-\frac{R}{\rho}\right) - \frac{e^2}{4\pi\epsilon_o}\left(\frac{1}{R} + \frac{\alpha'_A + \alpha'_{B(-)}}{2R^4} + \frac{2\alpha'_A\alpha'_{B(-)}}{R^7}\right) \quad (34)$$

which excludes the very small van der Waals contribution. This reduces the usual number of parameters by two, making the total number of input data four, i.e., one less than that of the pVSAM model. The Rittner model is limited to ionic molecules, where a cation and an anion can be uniquely identified. Therefore, for certain classes of heteronuclear molecules, the application of the Rittner model is prohibited, as may be exemplified by the alkali-metal hydride molecules. The H^- ion polarizability, $\alpha'(H^-)$, is far too large to fulfill the requirement that $\alpha' < (4\pi/3)R_e^3$, and the polarizability of a partially charged negative ion ($H^{\delta-}$) is not even defined. Therefore, the Rittner model is applied only to the halides. In calculations for these metal halides, the A^+ polarizabilities in Table 1 (presented later in this paper), and the B^- anion polarizabilities, as given in Rittner's paper,[8a] were used.

2.5. Operational Parameters $D_{VS}^{(\alpha)}$ and $G^{(\alpha)}$. Unlike input parameters such as k_e and R_e, which are taken directly from the experimental data, the value of D_{VS} and, by extension, q and z are dependent on the amount of hybridization/promotion assumed in the calculation. An operational dissociation energy $D_{VS}^{(\alpha)}$ has thus been defined,[3,4,11] which is determined by fitting the PEC to the observed $F = \alpha_e\tilde{\nu}_e/6B_e^2$ (see eq 27). Spin-orbit and relativistic effects, and lone-pair interactions impact on the potential energy curve and the promotion energy. The influence on the latter is assessed by the difference between the D_{VS} and the operational VS dissociation energy, $D_{VS}^{(\alpha)}$. For the VS-PEC,[4] it has been shown[11] that

$$D_{VS}^{(\alpha)} = \frac{k_e R_e^2}{3F} = \frac{hcB_e\tilde{\nu}_e}{\alpha_e} \quad (35)$$

We found, for the VS-PEC, that $D_{VS}^{(\alpha)} \approx 1.02D_{VS}$ for a representative set of 45 diatomic molecules.[4,5] By substituting for $D_{VS}^{(\alpha)}$ in eq 5, the related operational $VSAM_\alpha$ values of $T^{(\alpha)}$ and $z^{(\alpha)}$ are determined. The evaluation of the operational input parameters allows for an estimation of the reliability of a given potential function by comparing the observed G value and the calculated $G^{(\alpha)}$ value for a given molecule. By similarly fitting the pVS_α PEC to F, we have now determined the relevant $D_{VS}^{(\alpha)}$ values.

It has been reported that, because of the effects of lone-pair interactions in halogen diatoms, the VS-PEC gives poor fits, especially for F_2.[3−5] These complications are bypassed here through the use of operational $D_{VS}^{(\alpha)}$ values for the four halogen diatoms.

TABLE 1: Cationic Polarizability Volumes

A^+ ion	α'_A (Å^3)[a]	B^+ ion	α'_B (Å^3)[b]
Li^+	0.0285	F^+	0.260
Na^+	0.148	Cl^+	1.46
K^+	0.817	Br^+	2.17
Rb^+	1.35	I^+	3.82
Cs^+	2.34		
Cu^+	1.03		
Ag^+	1.42		
Au^+	1.89		

[a] For α'_A, alkali-metal ion values taken from ref 28, and coinage-metal ion values are taken from ref 29. [b] B^+ polarizability volumes taken from ref 30.

3. Results and Discussion

The recommended polarizability volumes of metal and halogen cations, and the input parameters needed for generating the pVS-PECs, are listed in Tables 1 and 2, respectively. The dipole polarizability of H^+ is, of course, zero. Note that some of the Cs_2 data from refs 23 and 24 are erroneous; as already done in ref 5, we use the R_e, B_e, and α_e values of ref 32.

The values of z, q, and $q_{c,eff}$, evaluated from eqs 21−23, are listed in Table 3 for the cases (i) without polarization contributions (VSAM) and (ii) with polarization (pVSAM). In the case without polarization (VSAM), the values may be calculated either from eq 5 (i.e., the method outlined in refs 3−5 for calculating z, and then q from eq 13), or based on eqs 21−23 (by setting the polarization terms to zero).

3.1. Bond-Charges. Because the polarization terms contribute to the depth of the potential well (see eqs 18−20), their inclusion reduces the bond-charge needed to reproduce the experimental dissociation energy. With the exception of CsCl, for which a value of $q = 1.153$ is obtained, the VSAM bond-charges do not exceed $q = 1$. The inclusion of polarization reduces the CsCl bond-charge to $q = 0.947$. Here, the shift in the magnitude of the bond-charge is an important feature of the pVSAM, because a VSAM result that gives a value of $q > 1$ requires the unwarranted involvement of metal-ion subvalence orbitals.

The value of q correlates with the position of atoms in the periodic table and the bond order, with the average values and standard deviations for the pVSAM model being $q = 0.481 \pm 0.006$ e for Li_2−Cs_2, $q = 0.489 \pm 0.004$ e for the group 1 and group 11 hydrides, $q = 0.690 \pm 0.086$ e for the group 1 halides, and $q = 0.590 \pm 0.011$ e for the group 11 halides (see Table 3). A correlation between bond-charge and bond order has been identified by Parr et al.[14b,c] in their SBC model. The similarity in q for related molecules is not surprising, because it reflects the near equivalence in bond order of the molecules. Obtaining transferable bond-charge increments would be most gratifying for (i) future links to molecular mechanics and (ii) in the modeling of the electrostatic potential of molecules.

The trends in the effective bond-charges ($q_{c,eff}$; see Table 3) evaluated for the VS-PECs and pVS-PECs are consistent with chemical intuition. As molecules become more polar, charge

TABLE 2: General Input Parameters (R_e, k_e, D_e), Valence-State Dissociation Energy (D_{VS}), and Partial Charge (δ)[a]

molecule	R_e (Å)	k_e (eV Å^{-2})	D_e (eV)	D_{vs} (eV)	δ
H_2	0.7414	35.94	4.747	11.17	0
Li_2	2.673	1.576	1.056	3.44	0
Na_2	3.079	1.071	0.735	3.04	0
K_2	3.924	0.613	0.552	2.50	0
Rb_2	4.210	0.521	0.495	2.34	0
Cs_2	4.648	0.434	0.450	2.16	0
Cu_2	2.220	8.24	2.08	5.33	0
Ag_2	2.530	7.40	1.67	4.81	0
Au_2	2.472	13.29	2.32	5.78	0
F_2	1.412	29.51	1.66	6.50[b]	0
Cl_2	1.987	20.13	2.514	9.71[b]	0
Br_2	2.281	15.40	1.991	8.48[b]	0
I_2	2.666	10.76	1.556	6.70[b]	0
LiH	1.596	6.41	2.52	5.93	0.473
NaH	1.887	4.88	1.97	5.26	0.498
KH	2.240	3.52	1.83	4.64	0.571
RbH	2.367	3.21	1.81	4.52	0.587
CsH	2.494	2.92	1.84	4.37	0.615
CuH	1.463	13.85	2.85	7.31	0.279
AgH	1.618	11.46	2.39	6.78	0.286
AuH	1.524	19.74	3.13	7.97	0.143
LiF	1.564	15.48	6.00	7.82	0.822
LiCl	2.021	8.90	4.86	6.45	0.784
LiBr	2.170	7.43	4.37	6.15	0.749
LiI	2.392	6.00	3.57	5.61	0.712
NaF	1.926	10.99	4.98	6.59	0.844
NaCl	2.361	6.87	4.29	5.68	0.814
NaBr	2.502	5.83	3.82	5.40	0.781
NaI	2.711	4.76	3.18	5.03	0.746
KF	2.171	8.62	5.14	6.05	0.913
KCl	2.667	5.31	4.40	5.08	0.909
KBr	2.821	4.61	3.94	4.86	0.883
KI	3.048	3.82	3.40	4.60	0.853
RbF	2.270	8.04	5.20	5.96	0.928
RbCl	2.787	4.88	4.39	4.91	0.93
RbBr	2.945	4.32	4.01	4.79	0.905
RbI	3.177	3.60	3.44	4.50	0.876
CsF	2.345	7.60	5.32	5.80	0.954
CsCl	2.906	4.67	4.59	4.83	0.968
CsBr	3.072	4.08	4.09	4.60	0.946
CsI	3.315	3.39	3.48	4.28	0.919
CuF	1.745	21.01	4.43	7.99	0.642
CuCl	2.051	14.54	3.95	7.13	0.545
CuBr	2.173	12.99	3.45	6.75	0.497
CuI	2.338	10.97	3.00	6.46	0.447
AgF	1.983	15.78	3.64	7.09	0.651
AgCl	2.281	11.66	3.24	6.33	0.556
AgBr	2.393	10.59	3.00	6.21	0.508
AgI	2.545	9.21	2.60	5.98	0.458
AuF	1.938	18.4	3.3	7.8	0.526
AuCl	2.199	16.4	3.13	7.01	0.391
AuBr	2.318	14.7	2.96	6.77	0.334

[a] Note: 1 eV Å^{-2} = 0.1602 mdyn Å^{-1}. R_e, k_e, and D_e values are obtained using data from refs 23 and 24 or are taken from refs 3, 4, 5, and 11, from where the "ansatz" for D_{VS} was also adopted. For Rb_2, R_e, D_e, F, and G values are taken from ref 31. Some Cs_2 data from refs 23 and 24 are erroneous; we have used those from ref 32. Reference 33 is the source for AuF, and ref 34 is the source for AuCl and AuBr. For Cu_2, D_e and G are taken from ref 35. Partial charge (δ) values are taken from ref 9 or calculated according to ref 9. Hybridization energies (E_{hyb}) and J values used are those given by Bratsch.[36] [b] Operational $D_{VS}^{(\alpha)}$ values are used for the halogen diatoms. Those listed are derived from the pVSAM function. For the VSAM function, the related operational $D_{VS}^{(\alpha)}$ values are 11.27, 10.42, and 8.74 eV for Cl_2, Br_2, and I_2, respectively.

accumulates at the more electronegative atom and the $q_{c,eff}$ value diminishes. The results for the alkali-metal halides and hydrides support this interpretation for both the VS-PEC and the pVS-PEC, with the exception of RbH and RbF, where the $q_{c,eff}$ values

TABLE 3: Dimensionless Valence-State Parameter (z) and Bond-Charge[a] Values

	VS-PEC			pVS-PEC		
molecule	z	q (e)	$q_{c,eff}$ (e)	z	q (e)	$q_{c,eff}$ (e)
H_2	1.768	0.517	−0.731	1.768	0.517	−0.731
Li_2	3.271	0.472	−0.668	3.278	0.472	−0.667
Na_2	3.338	0.480	−0.679	3.360	0.478	−0.676
K_2	3.776	0.491	−0.694	3.789	0.488	−0.689
Rb_2	3.949	0.488	−0.690	3.946	0.483	−0.683
Cs_2	4.333	0.490	−0.693	4.276	0.484	−0.684
Cu_2	7.616	0.535	−0.757	6.286	0.499	−0.705
Ag_2	9.848	0.536	−0.757	7.946	0.494	−0.698
Au_2	14.06	0.612	−0.866	10.26	0.541	−0.765
LiH	2.753	0.494	−0.615	2.782	0.492	−0.613
NaH	3.304	0.493	−0.604	3.348	0.489	−0.599
KH	3.806	0.496	−0.575	3.840	0.483	−0.561
RbH	3.979	0.512	−0.586	3.984	0.494	−0.565
CsH	4.156	0.518	−0.577	4.111	0.490	−0.547
CuH	4.054	0.529	−0.718	4.027	0.484	−0.658
AgH	4.425	0.534	−0.724	4.212	0.488	−0.661
AuH	5.750	0.572	−0.800	4.698	0.495	−0.692
LiF	4.842	0.620	−0.499	4.718	0.596	−0.480
LiCl	5.636	0.669	−0.587	5.139	0.616	−0.541
LiBr	5.689	0.685	−0.642	5.095	0.627	−0.588
LiI	6.119	0.669	−0.664	5.248	0.596	−0.592
NaF	6.186	0.624	−0.473	5.941	0.599	−0.455
NaCl	6.742	0.686	−0.563	6.135	0.639	−0.525
NaBr	6.758	0.682	−0.602	6.036	0.631	−0.557
NaI	6.955	0.677	−0.638	5.993	0.614	−0.578
KF	6.715	0.725	−0.418	6.246	0.656	−0.378
KCl	7.435	0.769	−0.454	6.762	0.689	−0.406
KBr	7.549	0.755	−0.501	6.770	0.680	−0.451
KI	7.715	0.760	−0.561	6.732	0.681	−0.502
RbF	6.951	0.832	−0.438	6.319	0.732	−0.386
RbCl	7.720	0.834	−0.434	6.960	0.728	−0.378
RbBr	7.822	0.848	−0.510	6.962	0.759	−0.456
RbI	8.075	0.816	−0.556	7.019	0.726	−0.495
CsF	7.206	0.946	−0.401	6.343	0.748	−0.317
CsCl	8.165	1.153	−0.409	7.218	0.947	−0.336
CsBr	8.370	0.979	−0.449	7.345	0.827	−0.379
CsI	8.704	0.869	−0.485	7.507	0.737	−0.411
CuF	8.010	0.658	−0.714	6.482	0.588	−0.638
CuCl	8.576	0.679	−0.805	6.561	0.603	−0.715
CuBr	9.091	0.670	−0.823	6.770	0.589	−0.723
CuI	9.283	0.685	−0.866	6.595	0.591	−0.748
AgF	8.749	0.660	−0.708	7.094	0.591	−0.635
AgCl	9.586	0.661	−0.777	7.449	0.589	−0.692
AgBr	9.764	0.676	−0.824	7.419	0.602	−0.733
AgI	9.974	0.686	−0.862	7.249	0.600	−0.754
AuF	8.9	0.71	-0.85_5	6.72	0.63	−0.76
AuCl	11.33	0.681	−0.886	8.102	0.593	−0.771
AuBr	11.69	0.686	−0.914	8.240	0.596	−0.794

[a] q, bond-charge increment; $q_{c,eff}$, effective bond-charge.

are slightly larger than those of KH and KF, respectively. For the group 11 metal halides, the value of $q_{c,eff}$ increases when one moves from fluorides to iodides. Moving down the group 11 halides, the $q_{c,eff}$ values for AuX are larger than the corresponding CuX and AgX values. This is rationalized by the very important relativistic effects at Au.

3.2. *F* and *G* Values. The values of F and G have been calculated from the energy derivatives for the energy function with and without polarization terms and are given in Tables 4 and 5, respectively.

The universality of the proposed ionic−covalent pVS potential function as a semiempirical model of chemical binding may be estimated from a comparison of the predicted F and G parameters with observed values. Such a comparison indicates the merit of the model by providing information on the behavior of the PEC within the vicinity of the minimum. The percentage

TABLE 4: Observed and Calculated Dimensionless Vibration−Rotation Coupling Constant (*F*) and Its Percentage Deviation from Experimental Values[a]

	F			*δF* (%)				
molecule	observed[b]	VSAM	pVSAM	VSAM	pVSAM	Morse	Rydberg	Rittner
H_2	0.6065	0.5894	0.5894	−2.8	−2.8	−27.1	−40.7	
Li_2	0.911	1.090	1.085	19.7	19.1	43.7	29.2	
Na_2	0.9680	1.113	1.097	14.9	13.4	68.2	52.7	
K_2	1.036	1.258	1.228	21.5	18.5	85.7	69.6	
Rb_2	1.080	1.316	1.279	21.9	18.5	111	93.8	
Cs_2	1.18	1.444	1.401	22	19	89	73	
Cu_2	2.29	2.539	2.263	11	−1.2	−7.3	−15	
Ag_2	2.63	3.283	2.848	25	8	5	−3	
Au_2[c]	(2.9−3.5)	4.686	3.705					
LiH	0.899	0.918	0.902	2.1	0.4	−11.0	−22.5	
NaH	1.112	1.101	1.070	−0.9	−3.7	−1.0	−11.8	
KH	1.201	1.269	1.196	5.6	−0.4	−0.4	−10.8	
RbH	1.236	1.326	1.230	7.3	−0.5	−0.6	−10.9	
CsH	1.229	1.385	1.254	12.7	2.1	−0.6	−10.9	
CuH	1.314	1.351	1.021	2.8	−22.3	−2.6	−12.5	
AgH	1.42	1.475	1.165	4.1	−17.8	6.2	−3.9	
AuH	1.565	1.917	1.460	22.4	−6.7	9.0	−0.9	
LiF	1.701	1.614	1.555	−5.1	−8.6	−54.4	−60.3	−26.7
LiCl	1.720	1.879	1.726	9.2	0.4	−45.7	−52.1	−15.4
LiBr	1.717	1.896	1.710	10.4	−0.4	−41.7	−48.4	−13.1
LiI	1.723	2.040	1.787	18.4	3.7	−30.8	−38.1	−8.2
NaF	2.132	2.062	2.003	−3.3	−6.0	−52.0	−57.4	−15.6
NaCl	2.084	2.247	2.107	7.8	1.1	−46.6	−52.4	−7.5
NaBr	2.070	2.253	2.083	8.8	0.7	−42.7	−48.8	−7.1
NaI	2.016	2.318	2.089	15.0	3.6	−33.3	−39.9	−3.6
KF	2.130	2.238	2.125	5.1	−0.2	−53.6	−59.0	−7.6
KCl	2.236	2.478	2.323	10.8	3.9	−52.1	−57.4	−3.2
KBr	2.363	2.516	2.338	6.5	−1.1	−51.0	−56.2	−6.7
KI	2.242	2.572	2.347	14.7	4.7	−42.7	−48.5	0.8
RbF	2.150	2.317	2.166	7.8	0.7	−53.7	−59.0	−4.8
RbCl	2.297	2.573	2.397	12.0	4.4	−53.1	−58.3	−2.1
RbBr	2.325	2.607	2.410	12.1	3.7	−50.0	−55.4	0.4
RbI	2.344	2.692	2.450	14.8	4.5	−44.6	−50.2	2.4
CsF	2.032	2.402	2.190	18.2	7.8	−51.7	−57.3	0.2
CsCl	2.318	2.722	2.500	17.4	7.9	−53.7	−58.8	2.8
CsBr	2.378	2.790	2.553	17.3	7.3	−50.8	−56.0	3.3
CsI	2.429	2.901	2.625	19.4	8.1	−45.9	−51.4	4.4
CuF	2.324	2.670	2.322	14.9	−0.1	−27.4	−34.0	−11.8
CuCl	2.2193	2.859	2.420	28.8	9.0	−19.7	−26.9	−6.3
CuBr	2.283	3.030	2.515	32.7	10.1	−13.2	−20.6	−3.5
CuI	2.330	3.094	2.493	32.8	7.0	−7.2	−15.0	−3.6
AgF	2.328	2.916	2.539	25.3	9.1	−17.6	−24.7	3.4
AgCl	2.2536	3.195	2.707	41.8	20.1	−8.6	−16.4	9.5
AgBr	2.336	3.255	2.719	39.3	16.4	−6.7	−14.5	9.0
AgI	2.417	3.325	2.699	37.5	11.6	−1.3	−9.3	6.0
AuF	2.47	2.97	2.47	20	0	−12	−19	0
AuCl	2.521	3.778	3.004	49.9	19.2	1.6	−6.5	10.3
AuBr	2.630	3.896	3.062	48.1	16.4	1.0	−7.0	9.6
			Average Error of Set[d]					
A_2[c]				**17.4**	**12.6**	**54.6**	**47.1**	
hydrides				**7.2**	**6.7**	**3.9**	**10.5**	
halides				**19.5**	**6.4**	**34.4**	**40.6**	**6.7**
overall				**17.1**	**7.5**	**32.6**	**36.6**	

[a] Signed percentage error evaluated according to the relation $\delta F\ (\%) = (F_{calc} - F_{obs}) \times 100/F_{obs}$. [b] Calculated using experimental spectroscopic data from refs 23, 31, 32, 37, and 38. [c] Au_2 is excluded from the average, because of the large uncertainty in the reference values. [d] Average unsigned percentage error, $\sum(|F_{calc} - F_{obs}|/F_{obs}) \times 100/n$, where n is the number of values in the relevant set.

deviation from experiment of the calculated *F* and *G* values from the VSAM, pVSAM, Morse,[21] Rydberg,[22] and Rittner[8] models are included in Tables 4 and 5, respectively.

The SBC model of Parr and Borkman[14b,c] is observed to give constant values—$F = 1$ and $G = 24$—for all molecules, in sharp conflict with the experiment. Therefore, this model is not listed in the tables. The erroneous prediction of constant values for *F* and *G* by the SBC model signals the difficulties of this model. The improved correlation that results from the VS-PECs and pVS−PECs, which also invoke the notion of bond-charge, indicates that the model proposed here does not simply follow from the original SBC model.

Except for the hydrogen molecule, where the core polarizability is zero and the VSAM and pVSAM values are equally excellent, the *F* and *G* values of the pVS-PEC are generally in better agreement with the experiment than in the case without polarization. For the alkali-metal dimers, the average unsigned errors show a consistent, albeit moderate, improvement with

TABLE 5: Observed and Calculated Dimensionless Anharmonicity Constant (*G*) and Its Percentage Deviation from Experiment[a]

	G			*δG* (%)				
molecule	observed[b]	VSAM	pVSAM	VSAM	pVSAM	Morse	Rydberg	Rittner
H_2	15.880	15.69	15.69	−1.2	−1.2	4.8	−3.9	
Li_2	31.0	29.8	29.7	−4	−4	37	26	
Na_2	37	30.5	30.3	−18	−19	48	36	
K_2	39	35.6	35.2	−11	−12	73	59	
Rb_2	49.7	37.1	36.5	−25	−27	73	59	
Cs_2	50	41.5	40.6	−18	−19	65	52	
Cu_2	76.1	87.4	75.8	15	−0.3	3	−6	
Ag_2	105	127	106	21	1	8	−1	
Au_2[e]	120, 208 ± 103	219	158					
LiH	24.67	24.58	24.47	−0.39	−0.83	5.1	−3.7	
NaH	31.22	30.1	29.8	−3.6	−4.5	13.0	3.6	
KH	35.2	35.5	34.5	1	−2	10	1	
RbH	36.91	37.4	36.1	1.4	−2.3	7.7	−1.3	
CsH	37.1	39.5	37.4	6	1	6	−3	
CuH	37.77	38.3	34.5	1.3	−8.8	10.1	0.9	
AgH	42.14	42.6	37.7	1.1	−10.4	19.1	9.2	
AuH	47.65	59.6	47.5	25.0	−0.3	22.9	12.7	
LiF	47.15	47.7	46.3	1.1	−1.8	−46.5	−50.9	−11.7
LiCl	51.0	58.0	53.5	14	5	−41	−46	−5
LiBr	55.9	58.7	53.3	5	−5	−43	−48	−11
LiI	61.2	64.7	56.7	6	−7	−37	−42	−14
NaF	64.0	65.6	63.7	2	0	−49	−53	−8
NaCl	65.2	73.8	68.7	13	5	−45	−50	−1
NaBr	62	74.0	67.9	19	10	−38	−43	4
NaI	65.5	77.0	68.5	17	5	−33	−38	0
KF	70.0	73.4	69.4	5	−1	−55	−59	−5
KCl	73	84.5	78.5	16	8	−53	−57	3
KBr	75	86.3	79.3	15	6	−50	−54	2
KI	75.4	89.0	80.0	18	6	−45	−49	5
RbF	72	76.9	71.5	7	−1	−56	−59	−2
RbCl	84	89.1	82.1	6	−2	−59	−62	−6
RbBr	77.9	90.7	82.8	16	6	−52	−56	6
RbI	81.6	94.9	85.0	16	4	−48	−53	5
CsF	70.3	80.9	73.0	15	4	−55	−59	1
CsCl	82.13	96.4	87.4	17	6	−58	−62	4
CsBr	83.0	99.9	90.0	20	8	−55	−58	7
CsI	86.1	106.0	93.8	23	9	−50	−54	7
CuF	83	93.8	79.4	13	−4	−30	−36	−10
CuCl	72	103	83.9	44	16	−14	−21	8
CuBr	83	113	88.8	36	7	−14	−21	−1
CuI	78.1	116	87.9	49	12	2	−6	7
AgF	78	107	89.9	37	15	−13	−20	13
AgCl	76.1	122	98.6	60	29	−2	−10	21
AgBr	85	125	99.3	47	17	−5	−13	13
AgI	82	129	98.5	58	20	12	3	18
AuF	85	109	87	29	2	−5	−13	9
AuCl	99.5	157	115	57	16	(2)[c]	−7	10
AuBr	105	164	119	56	13	(2)[c]	−7	9
			Average Error of Set[d]					
A_2[e]				**14.2**	**10.4**	**39.0**	**30.4**	
hydrides				**5.0**	**3.8**	**11.7**	**4.4**	
halides				**23.8**	**8.1**	**34.5**	**39.0**	**7.3**
overall				**18.9**	**7.8**	**31.4**	**31.7**	

[a] Signed percentage error, evaluated according to the relation $\delta G(\%) = (G_{calc} - G_{obs}) \times 100/G_{obs}$. [b] Calculated using experimental spectroscopic data from refs 23, 31, 32, 34, 37, 38, and 39; also see ref 40 for a recent review on the group 11 halides. [c] The anharmonicity constants of AuCl and AuBr in ref 34 are estimated using the Morse PEC; thus, the bracketed errors have been minimized by this fit. [d] Average unsigned percentage error, $\sum(|G_{calc} - G_{obs}| \times 100/G_{obs})/n$, where n is the number of values in the relevant set. [e] Au_2 is excluded from the average, because of the large uncertainty in the recent experimental values in ref 39d.

the observed *F* values. The bonding in these diatoms is very atypical, being weaker than the "one-electron bond" in the corresponding molecular ions A_2^+.[26] Most parametrized PEC models perform very poorly for the alkali-metal dimers.[1−5] The prevalent angular type of valence correlation has been invoked as a possible reason for the poor performance of the VS-PEC.[3,5] Even the inclusion of polarization does not address this problem. The error reduction in *F* and *G* is greatly enhanced for the coinage metal dimers, with, for instance, decreases of 17% in *F* and 20% in *G*, in the case of Ag_2. This is consistent with the experience gained from including a core-polarization potential in large-core pseudo-potential calculations on coinage-metal diatoms.[27] The polarization energy due to the static charge distribution is proportional to δ^2 and disappears for homonuclear

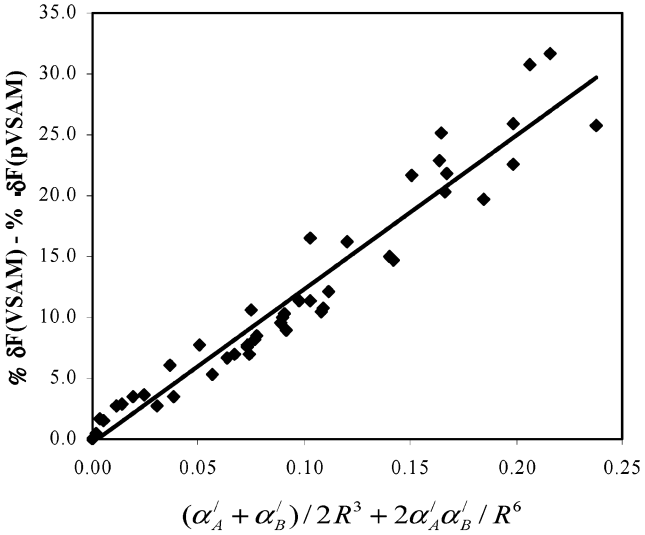

Figure 2. Differences between percentage deviations in *F* for valence-state-atoms-in-molecules (VSAM) and polarizable valence-state-atoms-in-molecules (pVSAM) models, as a function of the dimensionless parameter $(\alpha'_A + \alpha'_B)/(2R_e^3) + 2\alpha'_A\alpha'_B/R_e^6$. Correlation coefficient is $r = 0.965$, and the standard deviation is SD $= \pm 2.21$.

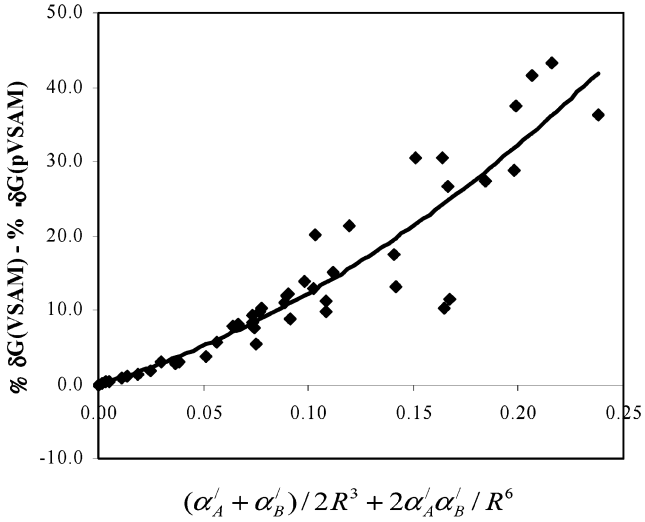

Figure 3. Differences between percentage deviation in *G* for VSAM and pVSAM, as a function of the dimensionless parameter $(\alpha'_A + \alpha'_B)/(2R_e^3) + 2\alpha'_A\alpha'_B/R_e^6$. Correlation coefficent is $r = 0.926$, and the standard deviation is SD $= \pm 4.51$.

diatoms; however, the presence of three structures in eq 6, and the polarizing bond-charge, relate to the dynamic charge distribution. The present polarization model is able to account for at least a portion of the dynamic core−valence correlation, because it goes beyond the static charge distribution.

Among the hydrides, there is an overall improvement in the correlation between *F* and *G* when polarization is included. The unsigned errors decrease from 7.2 to 6.7% in *F*, and 5.0 to 3.8% in *G*. The improvement, however, is somewhat uneven; for the subset of group 11 hydrides, we observe an increase of the average percentage error for *F* by 5.8% when polarization is added, whereas the errors in *G* are reduced by 2.6%. With the exception of NaH, there is a significant improvement in the value of *F* for each of the group 1 hydrides when polarization terms are included, and a slightly improved average error of 2.1% in *G* is observed. In the case of RbH and CsH, as earlier surmised,[5] the errors in the calculated *F* and *G* values for the VS-PEC are improved by taking core polarization into consideration. The different behaviors of the group 1 and group 11 hydrides may be attributed to a change in the reference VS energies by s,d orbital mixing in the latter subset.[27]

For the alkali-metal halides, the inclusion of the polarization terms results in a reduction by a factor of 3 in the average unsigned percentage errors for *F* (from 11.7% to 3.9%; see Table 4) and by a factor of 2 for the *G* values (from 12.6% to 5.0%; see Table 5). For the copper, silver, and gold halides, highly significant improvements in *F* (from 33.8% to 10.8%) as well as in *G* (from 44.2% to 13.7%) are observed. This gives an overall decrease in the unsigned error of 13.1% in *F*, and 15.7% in *G* for the group 1 and group 11 halides combined (see Tables 4 and 5). The strong improvement can be credited to the combination of large polarizabilities and short bond lengths for the metal halides. This general conclusion is supported by the correlations shown in Figures 2 and 3, which show the differences between the relative errors in *F* and *G* of the VS-PEC and the pVS-PEC, against the dimensionless parameter $(\alpha'_A + \alpha'_B)/(2R_e^3) + 2\alpha'_A\alpha'_B/R_e^6$. The plots illustrate the systematic improvement in accuracy of the pVSAM model over that of the VSAM model.

The plots include all the molecules except for the halogen diatoms, for which operational values are presented, and AuH and Au_2, which show exceptional behavior (see previous discussion). The same trend is observed if the differences between the absolute errors, δF(VSAM) − δF(pVSAM) and δG(VSAM) − δG(pVSAM), are considered. It has been noted that *G* itself is a quadratic function of *F*;[10] therefore, it is not surprising to find the quadratic dependence displayed in Figure 3.

Compared to the Morse, Rydberg, and Rittner functions, the pVS-PEC gives marked improvements in the accuracy of both *F* and *G*; the average errors become an order of magnitude smaller in many cases. In extreme cases, a comparison of the pVS-PEC with the Morse and Rydberg data for the alkali halides shows that the *F* and *G* values are improved by as much as 80% (cf. the averages for alkali halides in Tables 4 and 5). The Morse function performs surprisingly well for the group 1 hydrides and the group 11 dimers, whereas the Rydberg function is in relatively better agreement with the experiment for the group 11 hydrides and dimers (see Tables 4 and 5). Note the excellent performance of the Morse and Rydberg functions for the coinage-metal dimers: their δF and δG percentages are an order of magnitude smaller than those for the alkali-metal dimers. However, some authors more or less tacitly estimated some of the spectroscopic constants, using the Morse function; thus, small errors might be also due to such fits (cf. Table 5). In its limited range of applicability, the Rittner model is far more successful than the Morse and Rydberg functions (see Tables 4 and 5). The overall performance of the pVS-PEC is comparable to that of the Rittner PEC for the purely ionic subset of molecules. The performance of the Rittner PEC is very good for the group 11 halides, where the overall errors in *F* and *G* are slightly smaller that those computed for the pVS-PEC. By definition, the Rittner model includes the polarization by the static ionic charges only, which is the predominant effect in the extreme ionic limit A^+B^-. For $\delta \rightarrow 1$, the pVSAM model also converges to a purely static description of polarization.

3.3. Operational Parameters. For the halogen diatoms, several complications arise, which include the need to account for lone-pair interaction and problems associated with estimating the extent of the sp hybridization involved.[4,5] In the case of F_2, for instance, the bond length is short, the lone pairs of the two atoms are relatively close, and the repulsive interaction between

TABLE 6: Operational PVS_α-PEC Parameters and Calculated Anharmonicity Constants ($G^{(\alpha)}$)[a]

molecule	$D_{VS}^{(\alpha)}$ (eV)	$D_{VS}^{(\alpha)}/D_{VS}$	$z^{(\alpha)}$	$q_{c,eff}^{(\alpha)}$ (e)	$G^{(\alpha)}$	$\delta G^{(\alpha)}$ (%)
H_2	10.85	0.972	1.820	−0.698	16.13	1.5
Li_2	4.084	1.19	2.772	−0.842	24.6	−21
Na_2	3.420	1.12	3.007	−0.795	26.5	−29
K_2	2.915	1.17	3.302	−0.842	29.0	−27
Rb_2	2.724	1.17	3.449	−0.834	30.4	−39
Cs_2	2.538	1.17	3.717	−0.840	33.5	−34
Cu_2	5.259	0.987	6.366	−0.693	77.1	1
Ag_2	5.242	1.09	7.302	−0.778	94.1	−10
F_2	6.496		7.526	−0.471	96.3	−5
Cl_2	9.712		5.444	−1.048	76.6	−13
Br_2	8.484		6.343	−1.024	89.3	−15
I_2	6.701		7.553	−0.921	110.0	−16
LiH	5.950	1.00	2.773	−0.617	24.4	−1
NaH	5.084	0.966	3.454	−0.558	31.0	−1
KH	4.623	1.00	3.851	−0.556	34.7	−1
RbH	4.502	1.00	3.996	−0.560	36.2	−2
CsH	4.437	1.02	4.066	−0.566	36.7	−1
CuH	6.285	0.860	4.386	−0.500	41.1	9
AgH	5.943	0.877	4.559	−0.525	44.3	5
AuH	7.564	0.949	4.844	−0.642	50.7	6
LiF	7.183	0.919	5.108	−0.323	51.7	10
LiCl	6.471	1.00	5.125	−0.545	53.3	4
LiBr	6.128	1.00	5.110	−0.583	53.5	−4
LiI	5.799	1.03	5.111	−0.634	54.3	−11
NaF	6.197	0.940	6.315	−0.341	69.2	8
NaCl	5.742	1.01	6.071	−0.541	67.7	4
NaBr	5.435	1.01	5.999	−0.566	67.3	9
NaI	5.211	1.04	5.803	−0.624	65.4	0
KF	6.062	1.00	6.233	−0.382	69.2	−1
KCl	5.276	1.04	6.512	−0.473	74.5	2
KBr	4.809	0.989	6.843	−0.433	80.5	7
KI	4.816	1.05	6.435	−0.571	75.1	0
RbF	6.002	1.01	6.276	−0.400	70.8	−2
RbCl	5.122	1.04	6.672	−0.458	77.4	−8
RbBr	4.966	1.04	6.715	−0.516	78.8	1
RbI	4.707	1.05	6.713	−0.563	79.9	−2
CsF	6.235	1.08	5.908	−0.463	66.1	−6
CsCl	5.208	1.08	6.693	−0.483	78.7	−4
CsBr	4.938	1.07	6.841	−0.507	81.5	−2
CsI	4.629	1.08	6.942	−0.542	84.0	−2
CuF	7.979	1.00	6.487	−0.637	79.4	−4
CuCl	7.936	1.11	5.896	−0.830	73.4	2
CuBr	7.609	1.13	6.010	−0.849	76.5	−8
CuI	7.042	1.09	6.060	−0.836	79.1	1
AgF	7.774	1.10	6.497	−0.740	79.5	2
AgCl	7.831	1.24	6.041	−0.920	75.0	−1
AgBr	7.429	1.20	6.218	−0.920	79.0	−7
AgI	6.829	1.14	6.358	−0.890	83.3	2
AuF	7.907	1.00	6.725	−0.758	86.9	2
AuCl	8.682	1.24	6.514	−0.984	88.0	−12
AuBr	8.147	1.20	6.812	−0.975	93.8	−11
average[c]		**1.05**				**7.4**[b]

[a] The observed F values that were fitted to determine the operational values are given in column 2 of Table 4, except for the following halogen diatom (X_2) values: $F_{obs} \equiv 2.670$ for F_2, 2.350 for Cl_2, 2.563 for Br_2, and 2.918 for I_2. [b] Average unsigned percentage error in $G^{(\alpha)}$. [c] Au_2 is excluded from the list, because of the large uncertainty in the experimental F and G values (see Tables 4 and 5, respectively).

the lone pairs weakens the single bond. The impact of the lone pairs on the dissociation energy and other properties of the bond are not explicitly taken into consideration in the VS potential energy functions. Thus, the use of operational parameters provides an important route for a quantitative discussion of this group of molecules.

Following the treatment of the earlier results from the VSAM model,[3−5,11] operational VS dissociation energy values ($D_{VS}^{(\alpha)}$) have also been determined for all 47 molecules that have been already considered, and the halide dimers (X_2) (a total of 51 molecules; see Table 6). This is accomplished by fitting the observed F values as listed in Table 4. Numerically, this fitting is done by varying D_{VS} so that the right-hand side of eq 32 is equal to the observed F value. The operational dissociation energies and the related $G^{(\alpha)}$, $q_{c,eff}^{(\alpha)}$, and $z^{(\alpha)}$ values are listed in Table 6.

Having determined the operational pVS_α dissociation energy $D_{VS}{}^{(\alpha)}$ by fitting F, the difference between the operational and calculated dissociation energies is a direct reflection of how accurately the degree of hybridization was in determining the VS promotion energy. With an "ideal ratio" of 1.00, we find that, for the pVS_α PEC, the average $D_{VS}{}^{(\alpha)}$ value is $1.05D_{VS}$ for 47 molecules, for which D_{VS} was calculated directly from

promotion energies (i.e., all molecules except the halogen diatoms and Au_2).

The difference between the related $G_{VS}^{(\alpha)}$ and G_{obs} values provides an indication of the accuracy of the potential function. For the full range of molecules considered (except Au_2, which is excluded, because of the exceptionally large error bars in F_{ref} and G_{obs}), we find an average unsigned percentage error in $G_{VS}^{(\alpha)}$ of 7.4% (see Table 6). The pVS_α-PEC has a tendency to underestimate the anharmonicity constant G, when F is fitted, although the margin of error may be comparable to the error bar for G_{obs} in some instances. Based on eq 28, it is concluded that the fourth derivative at R_e is slightly overestimated by our model, when both the second and third derivatives are fitted to the experiment.

4. Summary and Outlook

The results for the alkali-metal and coinage-metal dimers, halides, and hydrides demonstrate the universality and merits of the polarizable valence-state-atoms-in-molecules (pVSAM) model. We have bridged the gap between the extreme ionic and covalent models of bonding by accounting for the three leading configurations, i.e., A^+B^-, A:B, and A^-B^+. The pVSAM model provides a rationale for configuration mixing, allows for bond-charge estimation, and includes higher-order effects up to polarization that is related to the dynamic core−valence correlation. Two ionic polarizabilities are added to the three molecular input parameters. The improved formalism leads to a consistently improved performance. The high information content of the valence-state dissociation energy (D_{VS}) is further established.

When polarization effects are added to the valence-state potential energy curve (VS-PEC), there is a 3-fold improvement in the calculated vibration−rotation coupling constant (F) and the anharmonicity constant (G) for a set of 48 molecules ranging from homonuclear to extremely ionic. The best results are observed for the group 1 and group 11 halides, where the relative error in F decreases from 19.5% to 6.4%, and that in G decreases from 23.8% to 8.1%. The overall performance is similar to that of the ionic Rittner model in its limited field of applicability and is 4-fold better than those of the Morse and Rydberg potentials.

Work is underway toward further evaluating and implementing the semiempirical polarizable valence state potential energy curve (pVS-PEC) through the following steps:

(i) Extending the analysis of pVS-PECs to the group 2 monohalides and hydrides. This series of molecules has been well-studied by a range of experimental and theoretical methods and will serve as an important testing ground for evaluating the applicability and limitations of the pVS-PEC.

(ii) Studying and utilizing the transferability of the bond-charge parameter q, as well as that of T and λ. We intend to establish links to molecular mechanics and calculate electrostatic potentials.

(iii) Applying a soft Coulson−Fischer transition,[5] to extend the range of validity to large distances ($R \rightarrow \infty$).

Acknowledgment. We thank Professors Hermann Stoll, Hans-Joachim Werner, and Michael Böhm, as well as Drs. Ratna Ghosh-Szentpály and Guntram Rauhut, for many helpful discussions.

Appendix. Contribution of the Covalent Component in the Potential Energy Function

With reference to Figure 1, the electric field at atom A is given as

$$E_A = \frac{q}{4\pi\epsilon_o(R/2)^2} - \frac{q}{4\pi\epsilon_o R^2} = \frac{3q}{4\pi\epsilon_o R^2} \quad \text{(A.1)}$$

The energy expression for the total Coulomb, charge-induced dipole, and induced dipole−induced dipole interactions between the atomic centers and the bond-charge fragments is given as

$$W_{cov} = -\frac{\alpha_A {E_A}^2}{2} - \frac{\alpha_B {E_B}^2}{2} - \frac{q^2}{4\pi\epsilon_o(R/2)} - \frac{q^2}{4\pi\epsilon_o(R/2)} + \frac{q^2}{4\pi\epsilon_o R} + \frac{2\alpha_A\alpha_B E_A E_B}{4\pi\epsilon_o R^3} \quad \text{(A.2)}$$

Because of symmetry, $E_A^2 = E_B^2$; thus,

$$W_{cov} = -\frac{3q^2}{4\pi\epsilon_o}\left(\frac{1}{R} + \frac{3(\alpha'_A + \alpha'_B)}{2R^4} - \frac{6\alpha'_A\alpha'_B}{R^7}\right) \quad \text{(A.3)}$$

References and Notes

(1) Varshni, Y. P. *Rev. Mod. Phys.* **1957**, *29*, 664.
(2) Steele, D.; Lippincott, E. R.; Vanderslice, J. T. *Rev. Mod. Phys.* **1962**, *34*, 239.
(3) von Szentpály, L. *Chem. Phys. Lett*. **1995**, *245*, 209.
(4) Gardner, D. O. N.; von Szentpály, L. *J. Phys. Chem. A* **1999**, *103*, 9313.
(5) von Szentpály, L.; Gardner, D. O. N. *J. Phys. Chem. A* **2001**, *105*, 9467.
(6) Zavitsas, A. A. *J. Am. Chem. Soc.* **1991**, *113*, 4755.
(7) (a) Murrell, J. N.; Sorbie, K. S. *J. Chem. Soc., Faraday Trans. 2* **1974**, *70*, 1552. (b) Huxley, P.; Murrell, J. N. *J. Chem. Soc., Faraday Trans. 2* **1983**, *79*, 323.
(8) (a) Rittner, E. S. *J. Chem. Phys.* **1951**, *19*, 1030. (b) Donald, K. J.; Mulder, W. H.; von Szentpály, L. *J. Chem. Phys.* **2003**, *119*, 5423.
(9) von Szentpály, L. *THEOCHEM* **1991**, *233*, 71.
(10) Freeman, G.; March, N. H.; von Szentpály, L. *THEOCHEM* **1997**, *394*, 11.
(11) von Szentpály, L. *J. Phys. Chem. A* **1998**, *102*, 10912.
(12) (a) Parr, R. G.; von Szentpály, L.; Liu, S. *J. Am. Chem. Soc.* **1999**, *121*, 1922. (b) von Szentpály, L. *Int. J. Quantum. Chem.* **2000**, *76*, 222.
(13) Ruedenberg, K. *Rev. Mod. Phys.* **1962**, *34*, 305.
(14) (a) Borkman, R. F.; Parr, R. G. *J. Chem. Phys.* **1968**, *48*, 1116. (b) Parr, R. G.; Borkman, R. F. *J. Chem. Phys.* **1968**, *49*, 1055. (c) Borkman, R. F.; Simons, G.; Parr, R. G. *J. Chem. Phys.* **1969**, *50*, 58.
(15) Sanderson, R. T. *Chemical Bonds and Bond Energy*; Academic Press: New York, 1980; p 10.
(16) Coulson, C. A.; Fischer, I. H. *Philos. Mag.* **1949**, *40*, 386.
(17) (a) Fuentealba, P.; Preuss, H.; Stoll, H.; von Szentpály, L. *Chem. Phys. Lett.* **1982**, *89*, 418. (b) von Szentpály, L.; Fuentealba, P.; Preuss, H.; Stoll, H. *Chem. Phys. Lett.* **1982**, *93*, 555.
(18) (a)Müller, W.; Flesch, J.; Meyer, W. *J. Chem. Phys.* **1984**, *80*, 3297. (b) Müller, W.; Meyer, W. *J. Chem. Phys.* **1984**, *80*, 3311.
(19) Pritchard, H. O.; Skinner, H. A. *Chem. Rev.* **1955**, *55*, 745.
(20) (a) Williams, D. E. *J. Comput. Chem.* **1988**, *9*, 745; **1994**, *15*, 719. (b) Larson, E. G.; Li, M.; Larson, G. C. *Int. J. Quantum Chem., Quantum Chem. Symp.* **1992**, *26*, 181. (c) Swart, M.; van Duijnen, P. Th.; Snijders, J. G. *J. Comput. Chem.* **2001**, *22*, 79.
(21) Morse, P. M. *Phys. Rev.* **1929**, *34*, 57.
(22) Rydberg, R. *Z. Phys.* **1931**, *73*, 376; **1933**, *80*, 514.
(23) Lide, D. R., Ed. *Handbook of Chemistry and Physics*, 79th ed.; CRC Press: Boca Raton, FL, 1999.
(24) Huber, K. P.; Herzberg, G. *Molecular Spectra and Molecular Structure IV: Constants of Diatomic Molecules*; Van Nostrand Reinhold: New York, 1979.
(25) Varshni, Y. P.; Shukla, R. C. *J. Chem. Phys.* **1961**, *35*, 582.
(26) von Szentpály, L. *Chem. Phys. Lett.* **1982**, *88*, 321.

(27) Stoll, H.; Fuentealba, P.; Dolg, M.; Flad, J.; von Szentpály, L.; Preuss, H. *J. Chem. Phys.* **1983**, *79*, 5532.
(28) Lim, I. S.; Laerdahl, J. K.; Schwerdtfeger, P. *J. Chem. Phys.* **2002**, *116*, 172.
(29) Kellö, V.; Sadlej, A. J. *Theor. Chim. Acta* **1996**, *94*, 93.
(30) Fraga, S.; Muszynska, J. *Atoms in External Fields*; Elsevier: Amsterdam, 1981.
(31) (a) Amiot, C.; Crozet, P.; Vergès, J. *Chem. Phys. Lett.* **1985**, *121*, 390. (b) Seto, J. Y.; Le Roy, R. J.; Vergès, J.; Amiot, C. *J. Chem. Phys.* **2000**, *113*, 3067.
(32) Vidal, C. R.; Raab, M.; Hönig, G.; Demtröder, W. *J. Chem. Phys.* **1982**, *76*, 4370.
(33) Schwerdtfeger, P.; McFeaters, J. S.; Liddell, M. J.; Hrusak, J.; Schwarz, H. *J. Chem. Phys.* **1995**, *103*, 245.
(34) Evans, C. J.; Gerry, M. C. *J. Mol. Spectrosc.* **2000**, *203*, 105.
(35) Rohlfing, E. A.; Valenti, J. J. *J. Chem. Phys.* **1986**, *84*, 6560.
(36) Bratsch, S. G. *J. Chem. Educ.* **1988**, *65*, 34.
(37) (a) Essig, K.; Urban, R.-D.; Birk, H.; Jones, H. *Z. Naturforsch.* **1993**, *48a*, 1111. (*F* value for LiI and *G* values for the alkali halides.) (b) Rusk, J. R.; Gordy, W. *Phys. Rev.* **1962**, *127*, 817.
(38) Simard, B.; Hackett, P.; James, A. M.; Langridge-Smith, P. R. R. *Chem. Phys. Lett.* **1991**, *186*, 415. (α_e and B_e for Ag_2.)
(39) Anharmonicity constants are taken from the following sources: (a) Krisher, L. C.; Norris, W. G. *J. Chem. Phys.* **1966**, *44*, 974 (for AgBr). (b) Rao, P. R.; Apparao, K. V. S. R. *Can. J. Phys.* **1967**, *45*, 2805 (for CuBr). (c) Manson, E. L.; De Lucia, F. C.; Gordy, W. *J. Chem. Phys.* **1975**, *62*, 4796 (for CuI). (d) Okazaki, T.; Saito, Y.; Kasuya, A. *Mol. Phys.* **1999**, *96*, 143 (for Au_2).
(40) Guichemerre, M.; Chambaud, G.; Stoll, H. *Chem. Phys.* **2002**, *280*, 71.